Mathematical Modelling of the Peloton

Mohit Vellore
Supervisor: Dr Stuart Thomson
Project Report submitted in support of the degree of Bachelor of Engineering

May 24, 2024

Abstract

Professional road cycling tests a rider's endurance and speed while also being a strategic battle among competitors within an aerodynamic environment. To combat the high physical demands of the race, riders form a peloton, where a group of riders ride together, minimising drag and increasing their energy expenditure efficiency. This formation is an example of cooperative behaviour in a competitive environment. Riders can choose to stop cooperating with others and break away from the peloton, thus, using this as a strategic move to disrupt the peloton's rhythm and give way to a race-winning lead.

In races and competitive situations, the assumption is that working with teammates and other competitors in certain situations allows for a better result amongst all those who cooperate. However, it remains unsure to what extent this assumption holds true and under which circumstances. It is also essential to understand when the switch between cooperation and competition needs to occur as switching from cooperation to competition too early can result in unwanted consequences. Other members could view the switch as hostile behaviour which could be punished by not allowing the hostile member to benefit from the cooperative behaviour. However, switching from cooperation to competition too late can result in other members taking advantage and benefiting from the extended cooperation to maximise their gain.

To explore this, our paper first investigates and establishes the need for cooperation to increase the probability of finishing a race first. We then utilise this behaviour and incorporate it within a cooperative model. We then expand on this and explore how non-cooperative behaviour affects the cooperative strategy and the means of maximising the probability of finishing a race first. Finally, we incorporate game theory into non-cooperative models to find an optimal strategy for switching between cooperative and competitive behaviours.

Our results show dynamic strategies leveraging cooperative and competitive elements can significantly increase performance and race-winning outcomes. With mathematical models such as the domestique model, we simulate specific strategic and scenario-dependent situations to demonstrate the interactions between members, giving insights that challenge traditional assumptions within a competitive environment. This report enhances our understanding of cooperative and competitive behaviours within games involving runners or cyclists whilst providing a broader perspective of competitive games in other sports.

This project did not require ethical review, as determined by my supervisor Dr Stuart Thomson.

Contents

1 Introduction

1.1 Motivation

In professional road cycling, maximising a rider's energy efficiency can win or lose a race. Phillips et al. discuss and highlight the impact of various physiological factors on competitive success,

with an important factor being a rider's energy efficiency [10]. One of the biggest influences on energy efficiency is drag, the resistance exerted by the air on the cyclist. To combat this, cyclists form a group called a peloton and ride together. Due to the structure of the peloton, cyclists take turns shielding each other from drag, a prime example of reciprocal altruism [11]. Reciprocal altruism is a cooperative strategy where individuals help others with the expectation of future benefits, similar to what occurs within the peloton. Each cyclist riding at the front of the peloton sacrifices their energy advantage for the group, expecting a similar concession from others, promoting a cycle of mutual benefit essential for enduring the race's demands. This behaviour parallels that seen in nature, an example of which can be seen in migrating birds, taking turns leading their formation to reduce fatigue and conserve energy for the group. This behaviour in nature and road cycling offers insight into the dynamics of cooperative strategies in competitive environments.

The tit-for-tat strategy can be observed within competitive environments. A specific example is within the peloton, where cyclists respond to the actions of others around them by either cooperating or retaliating. For example, suppose a cyclist avoids taking their turn at the front. Others may respond by excluding them from the protective draft - a direct form of competitive retaliation. This retaliation is due to behaviour that highly emphasises the importance of reciprocal cooperation. Conversely, cyclists who consistently contribute to the workload and exhibit cooperative behaviour are more likely to receive peer support when breaking away from the peloton, switching to a more competitive strategy.

Game theory is the natural mathematical language to explore tit-for-tat strategies in competitive and non-competitive environments [12]. By utilising game theory, we can mathematically formulate how interactions between other members are influenced by previous interactions within a group and individual conditions, hence, echoing the tit-for-tat mechanism's foundational role in promoting cooperation.

This project aims to better understand the dynamics at play within two-player games by exploring how cooperative and non-cooperative actions affect them and incorporating game theory. We chose the case of games involving two players as it allows us to better understand the principles behind the dynamics within a game. The insights gained from this study will allow us to find an optimal strategy for these games in various scenarios while being grounded in games involving runners or cyclists.

1.2 Previous work

This section reviews the foundational models, theoretical frameworks and other studies that helped shape our understanding of the cooperative and non-cooperative behaviours that occur in two-player games, with a particular focus on cycling. By understanding previous contributions and studies across different disciplines, we will establish the context of our investigation into the dynamics of cooperative and non-cooperative behaviour within two-player games and cycling.

Keller's research on optimal velocities in a race is at the centre of this report [2]. His analytical framework introduced a set of motion and energy conservation equations initially intended for runners. However, we can utilise these as a baseline for the models discussed in this paper. Keller's equations focus on maximising speed by optimising energy expenditure over a fixed distance, providing a theoretical guideline for achieving optimal race performance.

Stuart et al. extended Keller's principles to the context of cycling. They developed a model to determine the optimal timing and positioning for a cyclist to break away from the peloton, considering the interplay of drag and energy efficiency [3]. This application of Keller's equations to cycling shows the model's versatility for providing a baseline across different sports. Furthermore, it offers applicability and insights that can be gained from the tactics and behaviours found during a race. Martinon's work took a different approach by adapting Keller's model to the specific challenges of running on curved tracks [4]. This research accounts for the additional energy costs and biomechanical factors involved in maintaining speed on bends, thereby optimising performance strategies for athletes competing in races that include curved track segments. This extension of Keller's model highlights the potential to extend and develop the equations of motion and energy conservation initially proposed by Keller into more sophisticated equations specific to a desired application.

Agent-based models (ABMs) provide a robust framework for simulating complex interactions and strategies within competitive sports, with a focus on the cooperative and non-cooperative behaviours that emerge during sports. The paper by Railsback et al. explores how ABMs can conceptualise athletes as individual agents, each with distinct behaviours that interact dynamically with others [13]. This research highlights the utility of simulating the complex dynamics of competitive environments where multiple actors interact under varying conditions, allowing us to understand both the macro and micro dynamics that occur across various sports and within groups, such as a peloton.

Smith's review of ABMs within sports illustrates how the framework has been employed across various sports to analyse how individual and collective behaviours influence team performance and competitive interactions [5]. Smith's work highlights examples where ABMs have unravelled the underlying behaviours within team dynamics and between other competitors, particularly in sports where positioning and timing are crucial for success, thus, showcasing the adaptability and potential to extend the models to account for different sports or increasing complexity. The study conducted by Doe et al. explores how cyclists in a peloton make decisions that reflect a mix of competitive and cooperative strategies, impacting overall race dynamics and outcomes [6]. These decisions can range from drafting behind competitors to reduce aerodynamic drag to sudden breakaways that challenge the peloton's cohesion.

Together, these studies underscore the potential of ABMs to enhance our understanding of the behavioural dynamics during a race, with the potential to focus also within a group setting. The potential insights gained are crucial in understanding and developing strategies that balance individual efforts with surrounding members in competitive environments.

Game theory is pivotal in strategic decision-making during a race, particularly when defying a group or changing strategies. The study by Gaul et al. analyses a breakaway strategy in professional cycling through the lens of aerodynamics and game theory [7]. This research models the decision-making process of breaking away from the peloton, weighing the aerodynamic benefits of drafting against the potential advantages of leading a breakaway to maximise the likelihood of winning a race ahead of competitors. Whilst being grounded in a cycling context, the study introduces a game-theoretical framework that can be adapted to simulate various racing scenarios where an athlete must choose between cooperation for mutual benefit with others or being competitive, escaping the other athletes to gain a tactical edge. This framework quantitatively assesses the risks and rewards of shifts between cooperative and competitive behaviours and how they can affect race outcomes. Complementing this, Pitcher's research explores similar strategic interactions in middle-distance running. It focuses on how runners can optimally adjust their pacing and positioning relative to each other to maximise race performance and probability to win [8]. The findings from this paper offer insight into the balance between maintaining energy for the final sprint and strategically positioning in relation to competitors throughout a race. By applying the principles behind these models and the potential insights gained, we can better understand the complex interplay of group and individual strategies and behaviours in cycling and other sports.

1.3 Project aims and objectives

This project aims to adapt existing mathematical models and implement new ones to demonstrate the dynamics of cooperative and non-cooperative behaviours in two-player games. It concentrates on games involving runners or cyclists and uses the well-established Keller model as a basis. To achieve these aims, we set three key objectives. The first objective is to develop a model that accurately represents the equations of motion for a rider within the peloton, including the effects of drag reduction. The next objective is to model the balance between cooperation (reciprocal altruism) and competition (tit-for-tat) between riders and how these affect race outcomes. Finally, we use these models to propose optimal rider strategies depending on the scenario.

2 Method

In this section, we will explore the equations of motion and energy conservation for a cyclist, adapted from Keller's work, in order to form model equations suitable to complete our project aims [2]. We cover the analytical solutions found by Keller, using them as a baseline for our initial model and explain why it is better to opt for numerical solutions for our models. We then cover the collocation methodology, which is our choice for optimisation across all the models discussed in this paper, and how this is best placed for our objectives.

2.1 Mathematical model for single rider

First, we need to understand the behaviour of a singular cyclist. We form the equations of motion and energy conservation by using the equations from Keller's model, which considers the optimal velocity for a race for distance runners. Although Keller's model was not specifically designed for cycling or long-range races, we apply it here with the recognition that adapting it unchanged to cycling includes certain assumptions. Notably, Keller's model employs a linear dissipation term to account for internal resistance within the body during running. In this study, we retain the original linear dissipation term from Keller's model to maintain the model's generalisability across different scenarios involving both runners and cyclists, although a quadratic drag term to describe aerodynamic resistance would typically be more accurate in cycling. This generalised approach allows us to explore strategic behaviours in two-player games without tailoring the model exclusively to the specific dynamics of cycling. This assumption is a deliberate choice aimed at allowing broader application and comparative analysis across sports, acknowledging that while it simplifies the representation of resistance, it may only partially capture the nuances of aerodynamic drag in cycling.

As Keller describes, the equations of motion are,

$$\frac{dv}{dt} + \mu v = f \leq f_{max}, \tag{1a}$$

$$\frac{dx}{dt} = v. \tag{1b}$$

The equations (1a) and (1b) are derived from Newton's Second Law, which describes the motion of a cyclist in our model and an arbitrary player from a generalised viewpoint. Henceforth, we will infer any results regarding a cyclist as transferable to an arbitrary player for a general game. The term $\frac{dv}{dt}$ represents the cyclist's acceleration, while μ is the internal resistance to movement. The force per unit mass, f, exerted by the cyclist is subject to a constraint $f \leq f_{max}$ where f_{max} is the maximum force per unit mass that the cyclist can produce. This constraint highlights the physical limit of the cyclist's effort. Equation (1b) states that the rate of change of the cyclist's position x over time equals their velocity v. This relationship links velocity directly to the cyclist's displacement.

Next, Keller describes the energy conservation equation as,

$$\frac{de}{dt} = \sigma - fv. \tag{2}$$

Equation (2) calculates the rate of change of energy $\frac{de}{dt}$ for the cyclist. Here, σ represents the rate at which oxygen is supplied at by breathing. The term fv indicates the rate of energy expenditure, which depends on the force applied by the cyclist and their velocity. As described before, we assume the drag term felt by the cyclist is identical to that felt by a runner in Keller's work.

Due to the nature of the race, we can impose the following initial conditions for v and e,

respectively, which are used in solving the ODEs found in equations (1) and (2),

$$v(0) = 0, \tag{3a}$$

$$e(0) = e_0, \tag{3b}$$

where e_0 is the initial maximal energy reserve of the cyclist. We also impose a non-negativity constraint on the energy conservation ODE from equation (2),

$$e(t) \geq 0 \quad \forall t \geq 0. \tag{4}$$

This constraint ensures that the model's representation of a cyclist's physical capabilities remains valid, as it is physically impossible for the cyclist's energy levels to become negative. This is especially important when the cyclist is cycling at maximal effort. Keller discusses the importance of such constraints in maintaining the realism and applicability of mathematical models in representing endurance in athletic performances. We use the assumption in our calculations and all the models discussed further that the cyclist(s) know what true zero energy is and will exert themselves until they physically cannot continue doing so.

We now can form a relation between velocity, D as the distance covered and T the time to race with the equation,

$$D = \int_0^T v(t)dt. \tag{5}$$

Now that we have the equations for a cyclist, we can form the problem. The problem is to find $v(t), f(t)$ and $e(t)$ satisfying the equations of motion and energy conservation defined in equations (1) and (2) with initial conditions defined in equation (3) so that T defined in equation (5) is minimised. Equivalently, we can maximise D given T, which is explained later in this section.

Now that we have formed our problem, we can express it slightly differently to solve for $v(t)$. We can see that the equations of motion are coupled ODEs, meaning that $f(t)$ directly and indirectly affects the equations of motion. Hence, we can reformulate this problem as an optimal control problem.

An optimal control problem is a framework in which we optimise a control variable for a given system with state variables using an objective function. The objective function is the formula that defines the goal of the optimisation, a function that we aim to either minimise or maximise through a control variable. In our system, $v(t)$ and $e(t)$ are state variables describing the state of our system, while $f(t)$ is a control variable. Using the relation described in equation (5), we wish to maximise D given T. The objective function is usually expressed as a minimisation when we perform optimisations. Therefore, we wish to minimise $-D$ given T. For our optimisation, we use the direct collocation method.

While the direct collocation method effectively solves many optimal control problems, other approaches are available. Other common methods include the shooting method and the pseudo-spectral method as described by Kelly [14]. The shooting method starts with an initial guess

of the control variables and iteratively refines these guesses to meet the end conditions of the problem. This approach is straightforward but can be sensitive to the initial guesses made by the user. On the other hand, the pseudo-spectral method transforms the problem into one of optimising parameters over the entire period of interest. It does this by using polynomial functions to approximate the changes in both the control and state variables over time. This method, while highly accurate, is computationally intensive, making it suitable for problems where precision is critical. Each method has its advantages and is chosen based on the problem's specific requirements and the solution's desired accuracy. We discuss why the direct collocation method was chosen in the next section.

2.2 Direct collocation methodology

Due to the nature of the models we explore in this paper, we are choosing to use the direct collocation method to solve the system of ODEs found in equations (1), (2) and equations discussed in later sections. An analytical solution is not guaranteed as the models develop and become more complex. Therefore, by using a numerical method, we can ensure that we find a solution numerically. In numerical analysis, methods like the Euler method are commonly used for directly solving ODEs by step-wise integration. However, the direct collocation method differs as it is primarily used for solving optimal control problems by discretising these problems into a series of algebraic equations at specific points, known as collocation points. It approximates the state and control variables' trajectories using polynomial functions. This allows the method to evaluate the variables, whilst enforcing the system dynamics and constraints at the collocation points.

To validate the direct collocation method for our model, we perform a proof of concept by replicating Keller's scenario with the specific parameters e_0,f_{max},μ, and σ, as detailed in his study. By doing so, we can evaluate the results produced by the direct collocation method against those published by Keller.

Using the OpenOCL codebase in MATLAB, we applied the direct collocation method to the scenario as Keller described in his paper [1]. The results, illustrated in figure 1, confirmed that our model replicates Keller's findings, thus, demonstrating the method's accuracy in capturing the system's dynamics under study. These results are significant as they validate our methodological choice and demonstrate the model's reliability in predicting race profiles and outcomes under controlled parameters.

The results from the direct collocation optimisation are visualised in figure 1, which shows the force exerted by the cyclist over time and their resulting velocity. As seen, the force applied $f(t)$ is maintained consistently before it sharply drops, hence, indicating the point at which the cyclist's energy reserves are used. The velocity $v(t)$ remains stable until it decreases with the reduction in force. This signifies the critical point at which the cyclist can no longer sustain their maximal effort and must decelerate. The steep decline seen in the velocity of the cyclist towards the end of the race, also highlights the effect of physical constraints on endurance sports, where

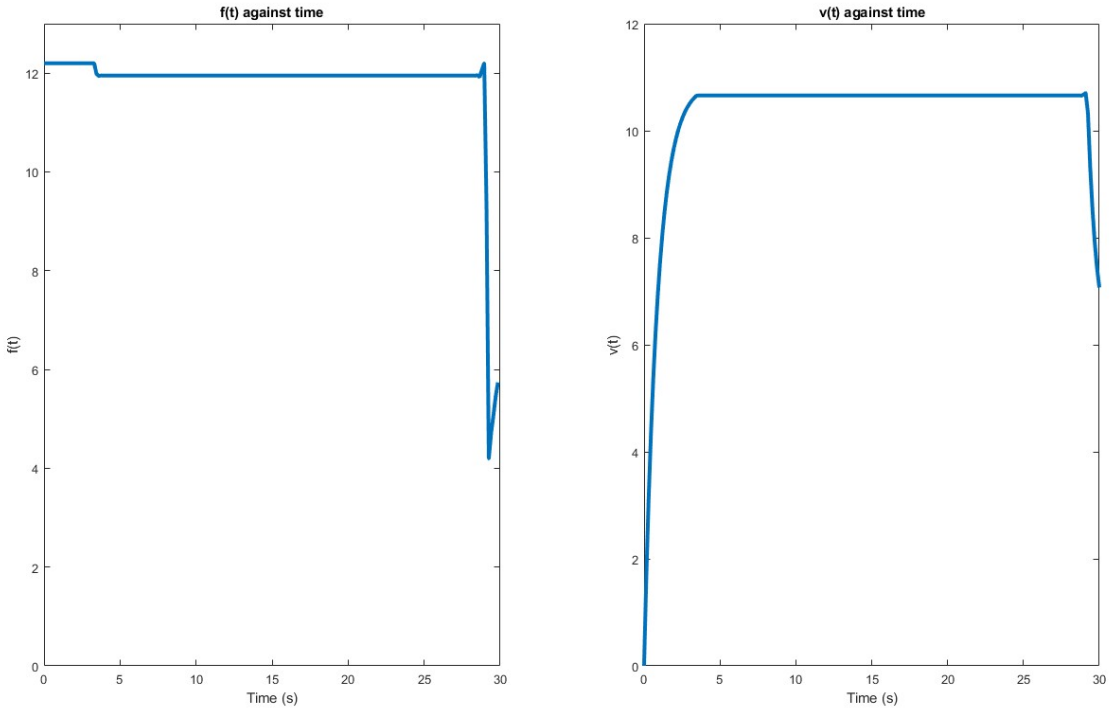

Figure 1: The plot on the left illustrates the force $f(t)$ applied by the cyclist over time, showing a sustained exertion level until a sharp drop, indicating the depletion of the cyclist's energy reserves. The plot on the right depicts the velocity $v(t)$ of the cyclist, which correlates closely with the force applied, maintaining a constant speed until the force can no longer be sustained, resulting in a rapid deceleration. Both plots were generated under the assumption of constant parameters: initial energy e_0, maximum force f_{max}, and physiological factors μ and σ as per Keller's original model.

athletes must strategically pace themselves to optimise performance throughout a race.

3 Co-operative Models

Having established a model for an individual rider, this section uses cooperative games from game theory to examine the dynamics of multiple riders interacting within a team setting. Initially, we analyse the interactions of two riders, A and B, which forms our study's simplest case and foundational base. This approach enables us to understand and demonstrate the principles behind rider interactions. While our current scope is limited to this two-player game, the model discussed in this section and further sections are designed with scalability in mind, allowing for future extensions to more complex cooperative dynamics - such as those found in a full peloton.

3.1 The Domestique

For the first model, we will explore the domestique's role and the dynamics that emerge from it. The domestique is a rider who works for the benefit of their team rather than trying to win the race. It's primary role is to protect the team from air resistance, sacrificing their energy levels to allow the team to finish faster. Alternatively, the domestique can also set a pace that strategically disadvantages competitors, benefiting the entire team in the long run, much like cooperative behaviours observed in nature. In our analysis, Rider A is the domestique, assisting Rider B to finish in the fastest time possible by optimising Rider B's performance and their likelihood of winning the race.

Rider B has the benefit of riding in the slipstream of Rider A, reducing the drag felt by Rider B, enabling energy conservation and sustained velocity with lower effort levels. This is because rider B requires a lower pedal force, $F(t)$, to maintain the same velocity, $V(t)$. While we maintain rider A's equations as previously established in equations (1) and (2), Rider B's equations of motion and energy conservation are captured by,

$$\frac{dV}{dt} + MV = F \leq F_{max}, \tag{6a}$$

$$\frac{dX}{dt} = V, \tag{6b}$$

$$\frac{dE}{dt} = \sigma - FV, \tag{6c}$$

The first equation (6a) represents the rate of change of velocity V for Rider B, where M is a function representing the air resistance felt by Rider B while in the slipstream of Rider A. The function M is visualised in figure 2 and examined later in this section. Just as with Rider A, F and F_{max} denote the pedalling force per unit mass and its maximal force amount produced by Rider B, respectively. The velocity V and the rate of energy expenditure $\frac{dE}{dt}$ are described by the subsequent equations (6b) and (6c), where σ remains consistent with the rate of energy supplied by breathing from Rider A's model.

Rider B's initial conditions and constraints are set analogously to Rider A's,

$$V(0) = 0, \tag{7a}$$

$$E(0) = E_0, \tag{7b}$$

$$E(t) \geq 0 \quad \forall t \geq 0. \tag{7c}$$

Rider B's energy $E(t)$ is constrained to always remain non-negative, thus, reflecting the physical reality that an athlete's energy levels cannot fall below zero.

As we see in equation 6, we have introduced a new term,

$$M = \mu\Theta(X - x) + \Theta(x - X)T(X - x), \tag{8}$$

where

$$\Theta(y) = \frac{1}{2}\tanh\left(\frac{y}{\epsilon}\right), \tag{9a}$$

$$T(z) = \mu(1-\gamma)[tanh(-wz) + \frac{\gamma}{1-\gamma}]. \tag{9b}$$

As mentioned above, the function M encapsulates the air resistance effect experienced by a cyclist cycling in the slipstream of another cyclist. We choose to retain the parameter μ from the single rider's equation (1) as the base resistance to movement. The drag reduction factor γ represents the percentage decrease in air resistance due to slipstreaming and is taken as approximately 0.7. In the study by Kyle et al., the various factors that affect cycling performance are discussed, including the benefits of drafting, which can significantly reduce air resistance [15]. While the literature varies on the exact numerical value for the benefit gained by cycling in a slipstream, we give an approximate value of 0.7, attempting to balance scepticism about the benefits gained while riding in the slipstream but also acknowledging that there is a noticeable difference in doing so. The drag reduction factor γ, when coupled with the base resistance μ, adjusts the air resistance to reflect the decreased energy expenditure for a cyclist drafting behind another.

The spatial parameter w, chosen as 2, defines the effective range in meters of slipstream benefit behind the domestique. Conversely, ϵ, set at 0.1, quantifies how sharply the slipstream advantage is lost when the rider is no longer directly behind the cyclist in the front, simulating the scenario where the slipstream effect diminishes swiftly. We can visualise the function M below,

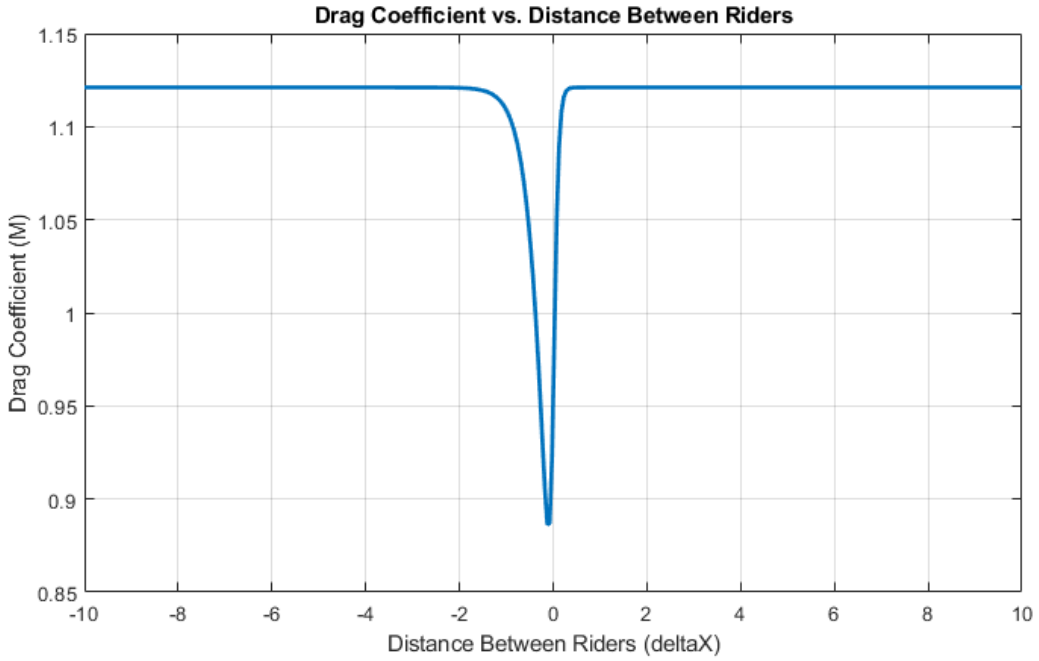

Figure 2: Plot visualising the air resistance function M with regards to distance between the riders.

As demonstrated in figure 2, the drag coefficient M decreases as the rider behind approaches the slipstream zone behind the rider in front, reaching its lowest when directly behind and sharply increases when an overtake occurs. This function is designed for scalability, dependent solely on the distance $X(t)$ between riders, thus allowing extension to models involving more riders without reliance on the control variable $F(t)$. Should the rider experiencing the slipstream move significantly ahead or fall far behind the rider at the front, we can express the following relationship for M,

$$\mid x - X \mid \to \infty \quad \text{then} \quad M \to \mu.$$

We can see that M asymptotically approaches μ, indicating the absence of slipstream benefits.

While we chose M to be distance-dependent, alternative formulations can be developed, relating M to riders' velocity or other variables. This allows the potential for further model complexity. However, these alternatives are beyond the scope of our study.

To determine the maximal distance covered by Rider B, we aim to maximise their velocity over time, represented as a negative integral. This objective function denoted as $\bar{D}$, is defined as,

$$\bar{D} = -\int_0^T V(t)dt, \tag{10}$$

where $\bar{D}$ represents the distance rider B covers.

The optimisation for Rider B incorporates the dynamics of both riders, as their motions are interconnected through the aerodynamic interaction between them, specifically the slipstream function M. In this cooperative scenario, Rider A does not seek to maximise their distance but rather to enhance Rider B's performance by minimising air resistance through strategic positioning. Therefore, our optimisation focuses on Rider B's distance to measure team success.

However, it is crucial to acknowledge that any optimisation for Rider B inherently affects Rider A due to the coupled nature of their equations. The effort and pace set by Rider A directly influence Rider B's energy conservation and velocity. Consequently, optimising Rider B's trajectory indirectly dictates Rider A's strategy, thus, ensuring that the domestique's efforts are effectively utilised for the team's advantage.

The optimisation for Rider B, solved using the direct collocation method, is depicted in Appendix A figure 7. These trajectories provide insight into the riders' velocity and energy conservation interplay. The analysis of the results shows that Rider A maintains a maximum output until 10 seconds, after which the rider begins to decelerate. At this point, Rider B capitalises on the energy conserved during the time spent in Rider A's slipstream. The resultant inflexion in Rider B's velocity curve reflects the increased effort required to overcome the sudden spike in air resistance once outside Rider A's slipstream. The advantage gained with this strategy is quantified by Rider B's total distance, showing a 43-meter increase compared to the results in figure 1 where the rider was cycling alone. This result confirms the traditional view that cooperative behaviour can increase performance within a sport. However, this statement is currently only valid for Rider B, as Rider A was a sacrificial player, and their performance was

sidelined.

3.2 Dynamic leading

We will further develop the domestique model and incorporate a more fluid strategy where the riders take turns leading. This model reflects a more sophisticated form of cooperation, where the traditional domestique role is expanded to include dynamic role-switching while still optimising rider B's performance. This model is more similar to that seen in professional level sports than to the domestique model, where riders take turns leading to maximise their overall energy efficiency.

The equations of motion for rider B remain unchanged. However, for rider A, the new equations of motion are as follows,

$$\frac{dv}{dt} + Mv = f \leq f_{max}, \tag{11a}$$

$$\frac{dx}{dt} = v, \tag{11b}$$

$$\frac{de}{dt} = \sigma - fv, \tag{11c}$$

where M is the function defined in equations 8 and 9. Our initial conditions and objective function remain unchanged. When we simulate our dynamic model, we get the results found in Appendix A figure 8.

The plots in Figure 8 reveal subtle periodic exchanges in the leading role. Contrary to the domestique model, dynamic switching allows both riders to distribute energy expenditure more evenly over the race duration, as the riders can benefit alternately from each other's slipstream, effectively employing a cooperative strategy to conserve and replenish both their energy levels.

Even though our optimisation objective prioritises Rider B's performance, the coupled nature of the cyclists' equations implies that any enhancement in Rider B's strategy indirectly benefits Rider A. As a result of this interlinked optimisation, Rider A can sustain a higher level of force and velocity during the race. The higher activity levels from both riders result in an improvement of 148 meters for Rider A, while Rider B gains an additional 24 meters compared to the domestique model results in figure 7. This indirect improvement for Rider A underscores the interconnection of cooperative dynamics, where optimising for one rider in a cooperative environment helps contribute to collective success.

The sharp transitions observed in the force output, particularly noticeable in Rider A's profile, raise questions about the numerical stability of our solution. This can be attributed to two key possibilities: the first is the solution not converging and numerical instability, and the other reason is due to the discretisation. We employed rigorous convergence checks within the direct collocation framework to ensure that these results did converge and that the sharp spikes were not due to numerical instability. We used convergence analysis, by running multiple simulation runs with refined time steps to confirm that these features are not artefacts of numerical errors but

genuine characteristics of the optimised strategy. To combat the effects of the discretisation that OpenOCL uses to compute the numerical solutions, we maximised the number of discretisations against the chosen numerical tolerance. We can then conclude that the volatile spikes seen in Rider A's profile are caused by the hardware being used not being able to handle a more significant number of discretisations.

3.3 Asymmetrical riders

To develop our model further, we will introduce the crucial complexity of resource asymmetry between the two players to account for the differences in the riders' max force output and initial energy levels, unlike the models discussed before.

To do so, we introduce α and β to quantify this resource asymmetry by defining Rider B's resources as a ratio of Rider A's, with the equations,

$$F_{max} = \alpha f_{max}, \tag{12a}$$

$$E_0 = \beta e_0. \tag{12b}$$

Here, α represents the ratio of rider B's maximum force output to rider A, while β represents the ratio between rider B's initial energy level and rider A's. These parameters are important since they help capture the variation between individual rider's physical capabilities but also the strategic potential each rider can bring to the race.

By dynamically adjusting α and β within our model, we can simulate a range of scenarios, offering insight into how teams can optimise their players' performances depending on the team's physical profiles. From this, teams looking to leverage individual strengths can strategise a more optimal race profile for their team's success.

We can plot a phase portrait to map out the conditions under which rider A or B will likely win, given the varying maximal force and initial energy levels dictated by α and β. The values of α and β only vary between one and a maximal ratio value. For our case, we choose the maximal ratio value of 2 to demonstrate the principles behind the cooperative dynamics between two players, each with physical strengths and weaknesses.

We can see in figure 3 that when both α and β are equal to 1, the result is a draw. This suggests that neither rider has a distinct advantage. As we vary these values, we notice different winning scenarios emerge, thus indicating the sensitivity of riders' relative capabilities against race outcomes. We see that the boundary between the regions where Rider A or Rider B is favoured delineates the critical values of α and β, serving as strategic inflexion points for race tactics.

As α increases to values up to 1.5, the ability of rider B to provide a longer slipstream for rider A is of greater value than being able to break away at a faster pace. This benefit depreciates until α has values greater than 1.5, where rider B's ability to break away faster always outweighs the

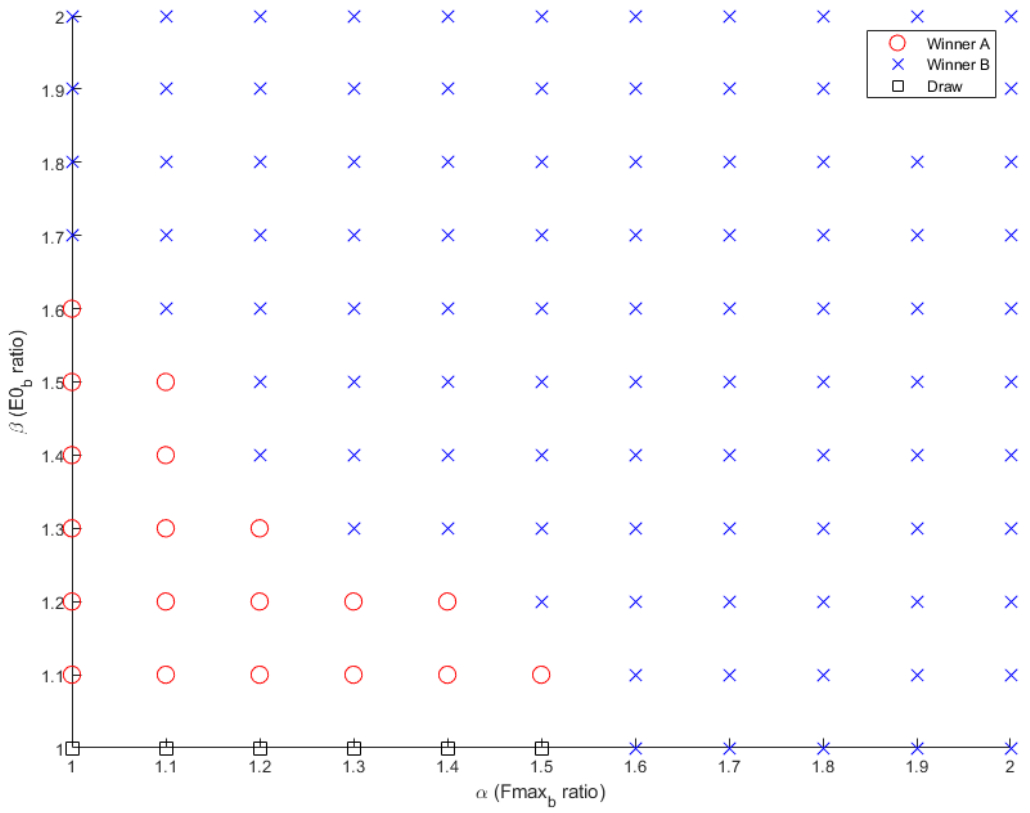

Figure 3: The graph illustrates the strategic outcomes of a cooperative race scenario between Rider A and B, with varying levels of maximal force F_{max} and initial energy reserves E_0. This variation is represented with a ratio with respect to Rider A's attributes. α and β, respectively, show the ratio values between max force and initial energy levels. Circles represent scenarios where Rider A is better placed, crosses where Rider B has the advantage, and squares indicate instances where either Rider is better placed to win a race. This figure highlights the relationship between resource asymmetry and race outcome, showing where the strategic inflexion points occur.

ability to provide a longer slipstream for rider A, always having rider B as being better placed to win.

For values of α between 1 and 1.5, maintaining β at a constant value of 1 results in a series of outcomes where neither rider is distinctly advantaged. We must note that a draw does not mean riders A and B have identical performances. Instead, the differences in their performances are not significant enough to determine an absolutely better-placed rider. Plotting distances both riders cover against the corresponding α values allows us to understand why these results occur.

We notice in figure 9, found in Appendix A, that as α increases, the overall distance covered by riders A and B increases. This suggests that Rider B's ability to produce more power is used towards maintaining a faster velocity during the race, hence, increasing the overall distance covered. To confirm this, the average velocities of riders A and B against the corresponding α values are plotted.

From the plot in figure 10, found in Appendix A, a slight upward trend is visible, similar to that seen in figure 9. This trend confirms that the maximal force rider B can exert over rider A increases their average velocity, albeit marginally. Due to rider B's greater force output, both riders contribute more effectively towards the team's pace since rider B's relative capacity improves. These results are seen in a subtle but consistent increase in collective velocity and distance covered.

4 Non-cooperative models

In this section, we will transition into non-cooperative models. Within a race, each player is both an ally and a rival, which reveals the subtleties of game theory. By analysing different scenarios, we explore the competitive nature of sports, highlighting the transitions between cooperation and competitive behaviour.

4.1 Stackleberg game

The first game theory case we will look at is the Stackleberg game. This is commonly found within economics, where decisions are made sequentially. The leader dictates the pace of the 'market', which in this case is the pace of the race, while the followers make their decisions afterwards, being aware of the leader's choice.

We take the Stackleberg game as our first scenario as it bridges our cooperative and non-cooperative models, to incorporate elements of both. The leader might make a strategic non-cooperative move, like breaking away or sprinting, in order to attempt an optimisation of their personal outcome without considering the other riders. The leader's decision could be influenced by the desire to gain an advantage, escape the group, or pressure competitors viewed as a threat. The followers must decide how to react to the leader's decision, whether to chase immediately, wait for others to react, or maintain a position within the group. This is a cooperative game, as the riders need to work together, sharing the effort to bring the leader back to the group.

For our first case, we will consider the scenario where Rider A is the leader and rides independently. In contrast, Rider B is the follower and has to react to Rider A. Rider A is aware that they are the stronger athlete and hence does not consider Rider B's actions. Rider B is aware that Rider A is the stronger athlete and takes this into account, looking to finish as close behind Rider A as possible to secure a second-place finish. Therefore, Rider B knows Rider A's position but not vice versa. For our model, we will take the values of rider B's maximal force output and initial maximal energy store to be exactly half of rider A's.

In figure 4, we can see Rider A having an identical race profile from when we optimised for a singular rider, as seen in figure 1. This is expected as Rider A is aware of their superior physical attributes. Meanwhile, Rider B maintains a more conservative approach. Rider B's force output starts at half of Rider A's and is maintained until the end of the race. Rider B's

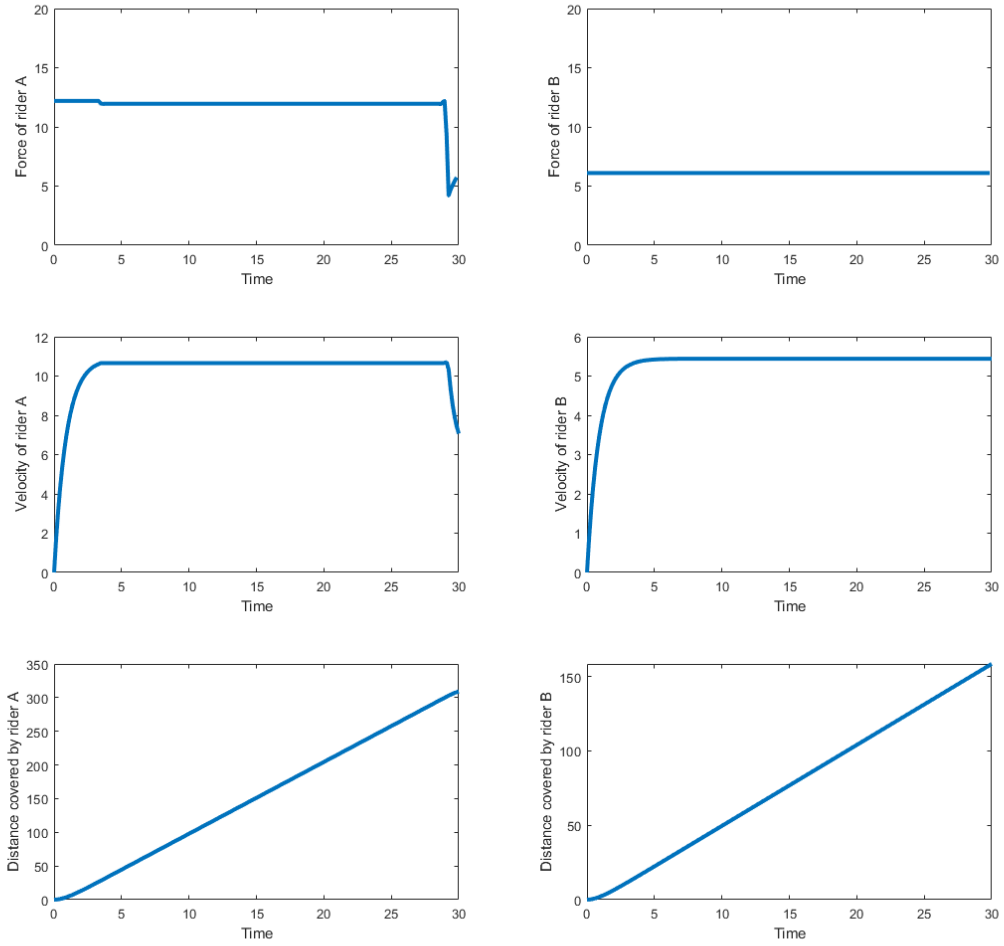

Figure 4: Comparative race profiles for Riders A and B in a strategy where Rider A leverages their superior physical attributes. The top graphs display force outputs for Rider A (left) and Rider B (right), with Rider A's force reaching a maximum and Rider B's starting at half that value. The middle graphs depict velocities for each rider, highlighting Rider A's aggressive pace versus Rider B's more conservative, energy-efficient approach. The bottom graphs show the distances covered over time, where Rider A achieves a significant lead. The model parameters, consistent with previous models, are chosen to reflect Rider A's dominance in physical capabilities, with Rider B's parameters set to half of Rider A's; $F_{max} = \frac{1}{2} f_{max}$ and $E_0 = \frac{1}{2} e_0$.

velocity maintains a lower steady pace than Rider A's, suggesting a more energy-efficient profile given the acknowledgement of Rider A's superior attributes. Overall, we can see that Rider A is unchallenged and rides independently of Rider B. At the same time, Rider B competes within their limits, looking to conserve their energy to ensure that they do not prematurely exhaust themselves whilst attempting to keep up with Rider A and finish the race as close to Rider A as possible.

We will now expand on our first case, changing some assumptions to build a more realistic

scenario. In this model, we will remain with Riders A and B looking to compete, with Rider B having half of Rider A's physical attributes. Rider A knows that they are the better athlete and rides independently, playing the role of the leader and Rider B as its follower. Rider B now acknowledges that Rider A might be the better athlete but remains unsure, causing Rider B to close the gap between themselves and Rider A but only if Rider B is within the distance that allows them to rider in the slipstream of Rider A. We will refer to this development on the previous model as an incentive function. We modelled the incentive function as such due to riders needing a slipstream to efficiently catch up and potentially overtake other riders during the race. It is unusual and often an exception for a rider to attempt to catch up to other riders without a slipstream due to the large energy requirement. We need to modify Rider B's equations of motion, as shown in equations 13.

$$\frac{dV}{dt} + MV = F + G \leq F_{max}, \tag{13a}$$

$$\frac{dX}{dt} = V, \tag{13b}$$

$$\frac{dE}{dt} = \sigma - FV, \tag{13c}$$

where M is the function defined in equations (8) and (9). Our initial conditions remain unchanged. G is the incentive function discussed above, with the formula shown in equation 14.

$$G = \begin{cases} \alpha^{-\beta|D_0 - D_1|(V_0 - V_1)}, & \text{if } D_0 - D_1 \leq 0 \\ -\alpha^{-\beta|D_0 - D_1|(V_1 - V_0)}, & \text{otherwise.} \end{cases} \tag{14}$$

In equation 14, α represents a scaling factor. The greater the value of α, the greater the responsiveness of the incentive to change the gap between the two riders. β gives a numerical value to the strength of the incentive to change the gap between the two riders, dependent on the changes in distance. For a larger β value, small changes in distance have a greater effect on the incentive of the rider, while for a smaller β value, small changes in distance have a smaller effect on the incentive. Therefore, a larger β value is suited for short races, and a smaller β value is suited for longer-distance races. D_0 represents the distance of the rider in front and D_1 represents the distance of the rider in the back. Similarly, V_0 is the rider's velocity in front, while V_1 is the rider's velocity in the back. For our model, we have chosen α to have a value of 0.8 and β to have a value of 0.2. This is suitable for our model, as the problem considers a long distance race, meaning a lower β value is more suitable than a larger one. We chose α to have such a large value as we want the incentive of the riders to be greater given that the race is over a long distance, having the incentive for the riders to last longer.

Introducing the incentive function into our model is a significant improvement, adding a layer of strategic complexity seen in real-race scenarios. This development focuses on the psychological elements of competition—an acknowledgement of an opponent's strength and the tactical decisions that stem from it. By quantifying Rider B's willingness to challenge Rider A based on proximity and slipstream potential, we bridge the gap between a more static race model and

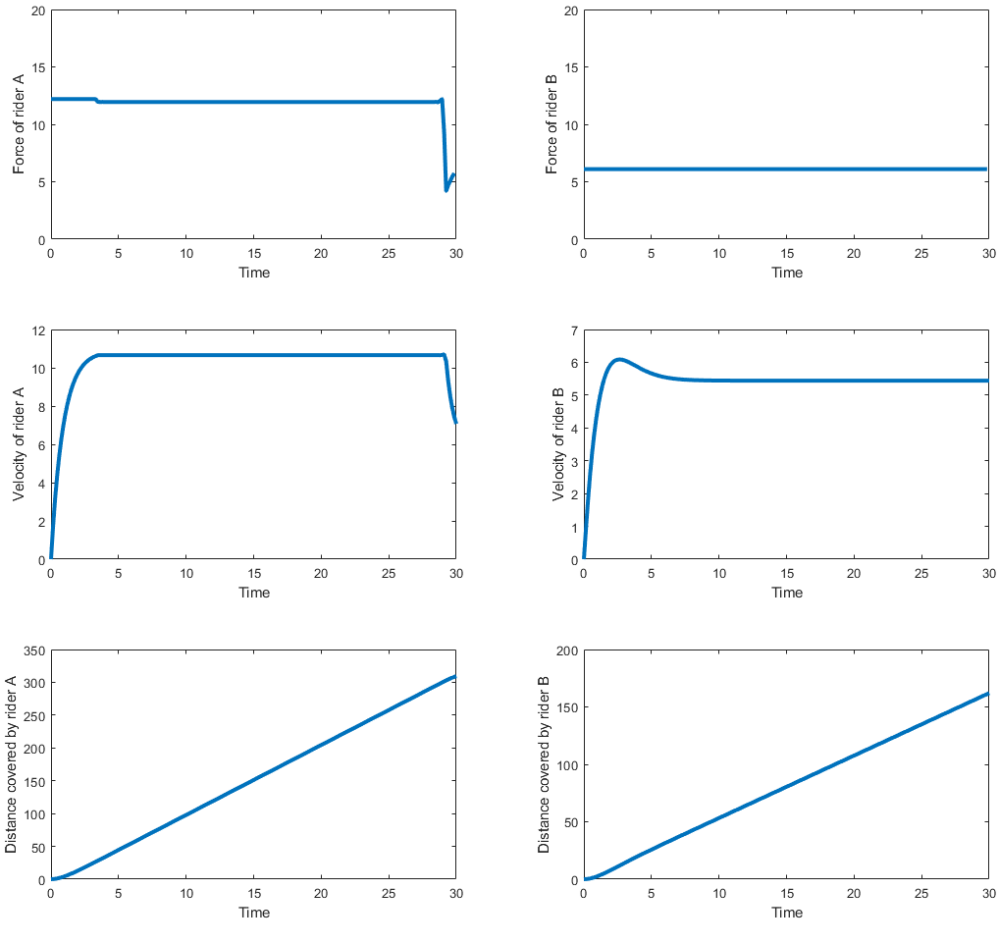

Figure 5: The plots present the race profiles of Rider A (left column) and Rider B (right column) under a scenario where Rider B is incentivised to close the gap to Rider A to utilise the slipstream. The top row illustrates the force exerted over time, the middle row shows velocity profiles, and the bottom row depicts the cumulative distance covered by each rider throughout the simulation. For Rider A, force and velocity are consistently high until a sharp decrease near the end, indicative of energy depletion. Having half of Rider A's physical attributes, Rider B starts with a lower force output but exhibits an increase when within the slipstreaming range of Rider A, demonstrating the incentive function's effect. As Rider B exits the slipstreaming range, the velocity drops, revealing the strategic impact of the slipstream on energy conservation. Parameters include a scaling factor (α=0.8) dictating the responsiveness of the incentive to the gap change and a strength factor (β=0.2) influencing the incentive magnitude based on the distance change.

one that mimics the dynamic decisions made by riders in response to evolving race conditions. This approach allows the optimisation to account for the psychological advantage, capturing how Rider B's uncertainty about Rider A's superiority influences their racing tactics.

As we anticipated, in figure 5, Rider A rides identically as in figure 4. However, the more active strategy of Rider B in figure 5 contrasted to their passive strategy in figure 4, showcases a

strategic change about by the incentive function. Initially, we observe a pronounced increase in force output and velocity from Rider B, which is a direct response to the proximity of Rider A and the opportunity to utilise their slipstream. This tactical choice demonstrates Rider B's drive to exploit the aerodynamic advantage and conserve energy, potentially positioning themselves to overtake Rider A as the race progresses. However, this increased output is short-lived, as seen by the downturn in the velocity profile. Once Rider A leaves the threshold from which Rider B is incentivised to ride at a higher pace, Rider B reverts to a more conservative energy management approach. This pivot in Rider B's strategy is a calculated response to the diminishing returns of pursuing a slipstream that is no longer within reach. We notice that Rider B has a notable increase in distance covered, highlighting the potential benefits of a dynamic racing strategy that adapts to the changing realities of the race rather than a static predisposed plan. Rider B's early race aggression, followed by a moderated pace, illustrates the balancing act between immediate exertion and long-term conservation. This nuanced strategy could yield a favourable outcome in a competitive setting where a rider is unsure of their competitor's superiority.

To expand on our model further, we will keep our previous assumptions the same. However, in this model, Rider A is riding independently and is now aware of Rider B's position and velocity relative to themselves. Rider A looks to increase the gap if Rider B is within a certain distance, which would allow Rider B to benefit from their slipstream. This model parallels a game of pursuit and evasion in game theory.

We need to modify Rider A's equations of motion, as shown in equations 15.

$$\frac{dv}{dt} + Mv = f + G \leq f_{max}, \tag{15a}$$

$$\frac{dx}{dt} = v, \tag{15b}$$

$$\frac{de}{dt} = \sigma - fv, \tag{15c}$$

where M is the function defined in equations 8,9 and 3.1, G is the function defined in equation 14. Our initial conditions and parameter values remain unchanged.

The results shown in figure 6 showcase race profiles closer to what is observed in actual races. The race starts with Rider A implementing a high-force output strategy and maintaining this consistent level of exertion as anticipated. However, as Rider B strategically drafts within the slipstream range, Rider A responds by increasing their effort levels to widen the gap and negate Rider B's aerodynamic advantage. This tactical response leads to a temporary spike in Rider A's velocity, indicating a successful breakaway and subsequent drop in Rider B's pace as they fall out of the slipstream. Throughout the race, Rider B's profile reveals intermittent increases in force and velocity, echoing Rider A's accelerative bursts. These profiles signify the dynamic interplay as Rider B attempts to regain the advantageous slipstream position.

At the end of the race, Rider A covered a greater distance compared to the previously discussed models in this section, with Rider B also achieving a notable increase in total distance. The increased velocity throughout the race can account for Rider A and B's increase in distance.

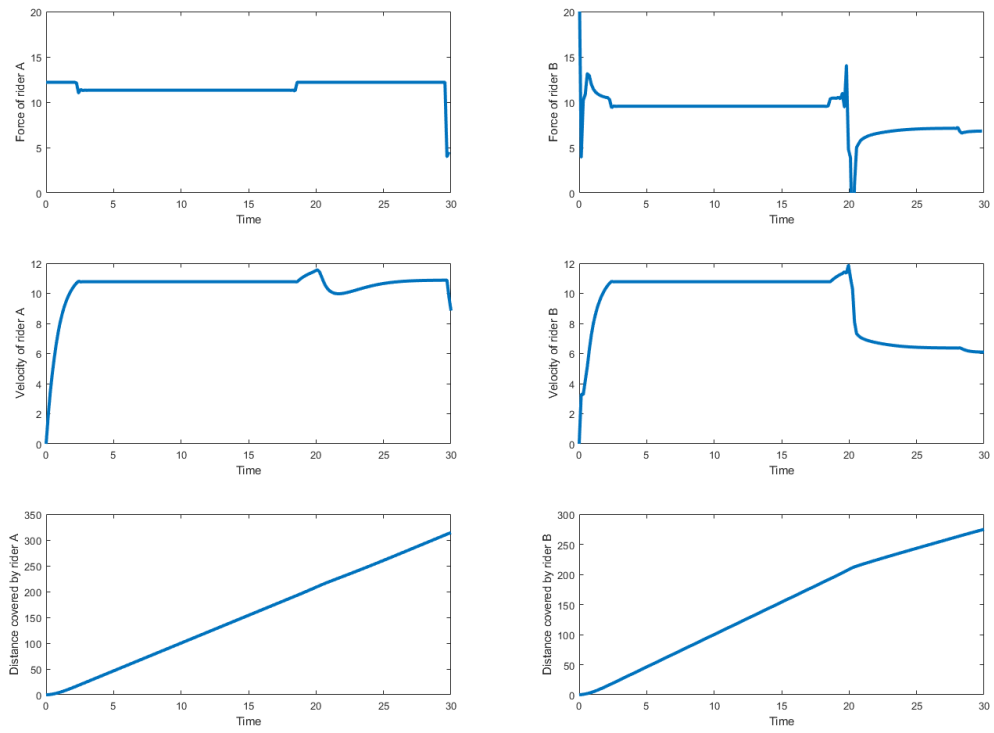

Figure 6: This figure presents the race dynamics between Rider A (left) and Rider B (right) under the modified incentive model, plotting force, velocity, and distance over the duration of the race. For Rider A, the constant high-force output with a prominent surge indicates a strategy to outpace Rider B, while Rider B's force and velocity exhibit reactive bursts in an effort to capitalise on Rider A's slipstream. The distance plots below reflect the result of these strategies, with both riders covering more ground than in previous models due to the competitive interplay. Model parameters include Rider A's superior physical attributes, with Rider B's force half of Rider A's; $F_{max} = \frac{1}{2} f_{max}$ and $E_0 = \frac{1}{2} e_0$.

Rider B did not cover as much distance as Rider A because of the increased energy expenditure during the race in an attempt to catch up to Rider A. When comparing profiles from figures 5 and 6, the current model highlights the strategic changes that occur during the race for Rider B. Rider B covers an additional 112 meters by using a more active strategy, attempting to stay in Rider A's slipstream for as long as possible, increasing Rider B's overall energy efficiency.

It is important to note once more that the volatile spikes in Rider B's force profile are caused by the discretisation that OpenOCL uses to compute the numerical solutions and suitable measures as stated before we used to negate these issues. Convergence analysis was conducted to confirm that these features are not artefacts of numerical errors but genuine characteristics of the optimised strategy.

4.2 Nash equilibrium

Our second scenario will look at the Nash equilibrium. In game theory, the Nash Equilibrium is a situation in which a player continues to carry out their strategy with no incentive to deviate from it after considering the opponent's strategy. In the context of our two-player games, Nash equilibrium is a set of strategies such that no player gains from unilaterally changing their strategy if the other player's strategies do not change. We can define the Nash equilibrium as follows,

$$U_A(A, B) \geq U_A(A^*, B), \tag{16a}$$

$$U_B(A, B) \geq U_B(A, B^*). \tag{16b}$$

Both U_A and U_B reference the set of strategies of riders A and B, while A^* and B^* signify the new strategy for riders A and B respectively. For this section, all relevant figures are found in Appendix A.

The Nash equilibrium is essential to understand as it provides a framework for how each rider's strategies interact with one another. With a thorough understanding, riders can better understand and decide when to exert maximum effort or conserve energy, thus identifying points at which their energy expenditure is optimised relative to the competition. It also allows for an equilibrium where both players cannot unilaterally switch to either a cooperative or competitive strategy to gain an advantage over the other player. Either player can tactically use their understanding of this equilibrium to enforce an advantageous position, forcing an unfavourable energy exchange for the opponent if they wish to contest the position. By doing so, each player has the potential to solidify their position at crucial points during a race by escalating their effort when they sense vulnerability or by conserving energy to contest when their opponent is looking to capitalise on any aggressive moves. This strategic interplay underlines the equilibrium as not just a point of mutual optimisation but also as a critical element in the psychological component of competitive sports.

Our optimisation approach for the models in this section deviates from what was used in previous models. Mathematically, we define our objective function, D, as the Nash equilibrium definition found in equation (16). However, due to the capabilities of OpenOCL, we had to break this minimisation into an iterative process, with the outline of the method shown in the pseudocode 4.2 below.

As each player's strategy depends on the other's, we had to first initialise a starting strategy for Rider B. For our model, we chose the distance covered by the rider as the comparison to check whether an improvement was made. We began by initialising Rider B's strategy based on the optimised values from the single rider model, scaled by a factor of $\Omega = 0.5$. This scaling is crucial as it positions our initial guess away from a non-responsive zero point, which could potentially trap the optimisation in a local minimum, hindering the attainment of a global solution. We then begin the iteration, optimising Rider A's strategy in the context of Rider B's current strategy, giving us $A_{optimal}$ in the pseudocode 4.2 and A^* in the definition found in equation (16a). Upon

Algorithm 1 Optimisation for Riders A and B to Reach Nash Equilibrium

$B_{\text{ini}} \leftarrow$ Initial values for Rider B
$B_{\text{values}} \leftarrow \Omega \cdot B_{\text{ini}}$ ▷ Scale initial values by factor Ω
Equilibrium_Reached $\leftarrow$ False
while Equilibrium_Reached = False **do**
    $A_{\text{optimal}} \leftarrow$ Optimise for A using B_{values}
    $B_{\text{optimal}} \leftarrow$ Optimise for B using A_{optimal}
    $A_{\text{test}} \leftarrow$ Optimize for A using B_{optimal}
    if A_{test} values are not significantly better than A_{optimal} **then**
        Equilibrium_Reached $\leftarrow$ True
    else
        $B_{\text{values}} \leftarrow B_{\text{optimal}}$
    end if
end while

obtaining an optimal strategy for Rider A, we optimise Rider B's strategy, considering the newly determined optimal strategy for Rider A, giving us $B_{optimal}$ in the pseudocode 4.2 and B^* in the definition in equation (16b). After re-evaluating Rider A's strategy with the updated strategy for Rider B, we find A_{test} denoted in the pseudocode 4.2. We use A_{test} to check for significant improvements against $A_{optimal}$ within a given tolerance. We introduced a tolerance of 10^{-5} to combat the numerical rounding during the optimisation process and avoid incorrect flagging of an equilibrium being reached. The absence of improvement suggests that a stable strategy has been reached from Rider A's perspective - one that Rider A has no incentive to unilaterally deviate from given Rider B's strategy. If a better strategy is found, we update Rider B's strategy accordingly and continue the iteration. Once convergence is achieved, meaning no further improvements can be made by either rider, it indicates that a Nash equilibrium has been reached. At this equilibrium, both riders have optimised their strategies given the actions of their competitor.

For our first model, we will let riders A and B have symmetric physical resources, $f_{max} = F_{max}$ and $e_0 = E_0$, where both riders will compete against each other to win the race. We will use the previously defined model in section 3.3, with $\alpha = 1$ and $\beta = 1$, as a benchmark for comparison, providing insights into how the dynamics of competition and cooperation alter race outcomes. Although the model defined in section 3.3 is cooperative, it mirrors results for non-cooperative games due to the ability to allocate resources asymmetry and indifference towards either rider during the optimisation. Rather than riders A and B being viewed as cooperators, they are now competitors, achieving the same results as if they were part of the same team.

In the Nash equilibrium model, both riders were assigned equal maximum force output ($f_{max} = F_{max}$) and initial energy levels ($e_0 = E_0$), competing directly to optimise their race outcomes against each other. Figure 11 shows the race profiles for each rider.

We will refer to the results from this model as 'Nash'. Riders A and B maintain the same velocity and force levels consistently throughout the majority of the race. However, the velocity and force exerted by each rider sharply decline towards the end of the race. As expected, the distance covered by both riders increases linearly over time. We can see that the profiles for

both riders are congruent in shape to those seen in the results from the single rider problem, figure 1.

As described in section 3.3, the asymmetrical riders model involved different resource allocations, with parameters $\alpha = 1$ and $\beta = 1$ signifying both riders have equal maximum force output ($f_{max} = F_{max}$) and initial energy levels ($e_0 = E_0$). Figure 12 shows the race profiles for each rider.

We will refer to the results from this model as 'Comparison'. Riders A and B maintain the same velocity and force levels consistently throughout the majority of the race. The velocity and force exerted by each rider sharply decline towards the end of the race, and the distance covered by both riders increases linearly over time. We see that once more, the profiles for both riders are congruent in shape to those seen in the results from the single rider problem, figure 1.

When we compare 'Nash' and 'Comparison', we notice that, overall, both race profiles have similar curves with subtle differences. In 'Nash', the force, velocity and distance covered by Riders A and B are slightly lower than that of Riders A and B in 'Comparison'. While this initially seems counterintuitive given that both models optimise for the same objective function of maximising their velocities. This discrepancy can be attributed to the nature of the Nash equilibrium and not numerical instability. To ensure that the differences seen are due to the nature of the Nash equilibrium and not numerical instability, we conducted convergence analysis, where we ran the simulation multiple times across a range of well-conditioned timesteps and compared the results.

In 'Nash', each rider's decision is predicted based on anticipating the other's choice. This reflects what occurs in races, as riders need to balance conserving energy and holding a steady speed whilst anticipating competitors' moves. This is shown in the velocity profiles of both riders in 'Nash', which is lower than in 'Comparison', where the riders in 'Nash' hold a more variable pace to maintain a position most beneficial relative to the other rider rather than solely optimising for a given objective. This is due to Rider A selecting a strategy based on the expected strategy of Rider B. Rider B selects their strategy with the knowledge of Rider A's approach. Neither rider can unilaterally change their strategy to improve their outcome without potentially benefiting the other rider. If Rider A were to pick a higher velocity unilaterally, there is no certainty that Rider B would follow suit and maintain a higher velocity. Rider B might instead decide to ride in Rider A's slipstream, benefiting from Rider A's decision. Therefore, both riders maintain a more variable velocity so that they can respond appropriately within their physical capabilities, leading to an overall lower velocity than in 'Comparison'. This leads to a lower distance covered by the riders than in 'Comparison'.

For our second model, we introduce resource asymmetry between riders A and B to investigate the impacts of unequal resource distribution in competitive strategies and outcomes. Specifically, Rider B will possess double the physical resources of Rider A, with $F_{max} = 2 \times f_{max}$ and $E_0 = 2 \times e_0$, reflecting a scenario where competitors have different physical capabilities or conditions. We maintain the same objective function, ensuring that any outcome differences can

be directly attributed to the resource disparity.

This approach allows us to explore strategic behaviours that emerge when competitors are not on a level playing field by examining how Rider A compensates for the resource disadvantage and how Rider B takes advantage of this.

We can see our models again from figures 13, which we will refer to now as 'Nash', and 14, which is now called 'Comparison'. There is a notable divergence in the results from the 'Nash' and 'Comparison' models, indicating that resource asymmetry is a significant factor in determining the best response strategy for each rider. Rider A is now using a more aggressive approach in the 'Nash' and 'Comparison' models to compensate for the resource disadvantage by attempting to ride in the slipstream of Rider B. However, in 'Nash' Rider B maintains a consistent pace similar to Rider A until the end, when there is an increase in velocity. This suggests that Rider B attempts to break away from Rider A at a time when Rider A does not have enough resources to contest the move and uses the resource asymmetry to its advantage by sprinting towards the end of the race. This is an example of a unilateral move from Rider B, which would improve their outcome without the risk of Rider A having the ability to mirror but choosing not to reciprocate to gain an advantage for themselves.

5 Conclusion

5.1 Results

In our modelling of the dynamics within the peloton, we employed both cooperative and non-cooperative models. These models helped us understand strategies players can adopt to optimise specific race outcomes, such as finishing the race as fast as possible. They also gave insights into how individual decisions within a group impact the player's overall performance and strategic positioning.

Our cooperative models showed a significant impact on the energy efficiency of a player. The Domestique model highlighted the effectiveness of the self-sacrificial role within a group, especially a team. By having a domestique, the lead rider's overall distance increased by 12%. Our Dynamic Leading model showed an increase of 15% in overall performance when riders alternated taking the domestique role, highlighting the importance of dynamic role switching within a cooperative environment. This is congruent with what can be seen in real race scenarios, with riders often switching positions to have better energy efficiency across all the members cooperating. The Asymmetrical Riders model further illustrated how teams can optimise performance by leveraging individual riders' strengths and physical attributes, strategising which rider is best placed to win the race.

Our non-cooperative models also showed how cooperation increases overall performance. However, the competitive dynamics between players introduce complexity, which alters race profiles and outcomes.

In our Stackleberg game models, we saw the dynamics between a leader and followers in a competitive environment. These models showed how a leader's strategy significantly influences the followers' strategies, forcing them to either conserve energy by riding in the slipstream or counter the leader's moves by using a large amount of energy. The leader's ability to impact the dynamics of the race was most prominent towards the end, where a sprint could disrupt the pace of the other riders. However, we saw that this came with the risk of early energy depletion. The models showcased how leaders balance their performance against the dynamics of the peloton.

The Nash equilibrium model showed a more life-like simulation of the competitive environment within sports, where each rider's strategy is made by anticipating the actions of the other riders, leading to a state where no individual rider can improve their performance by unilaterally changing their strategy without potentially creating a benefit for other riders. This model gave insight into the tactical stalemates within races, where players closely match each other's pace to conserve energy, waiting for a moment to make a decisive move. The Nash equilibrium model showed that a competitive environment naturally forms a stable equilibrium for the players under certain conditions, minimising overall energy expenditure whilst maximising the players' velocity. However, we see that this equilibrium is fragile, as resource asymmetry within the riders allows for a breakaway or a pace change from the stronger rider to disrupt the balance, thus, forcing a recalibration of strategies within the other riders.

5.2 Discussion

Our report on the dynamics of the peloton through both cooperative and non-cooperative models gave insights into the strategic behaviour implications of competitive environments. The report developed our current knowledge and provided significant understanding of the effectiveness of the domestique and dynamic leading strategies, enhancing team performance. These results support existing theories and studies on cooperative behaviour in competitive environments, aligning with the work of Smith et al. on team dynamics in endurance sports [5]. Our results extend to existing literature, quantifying the impact of these strategies under the objective functions defined in our models.

A traditional view is that a rider's individual strength is the predominant determinant of a race's outcome. Our results from the Stackleberg and Nash equilibrium models show that the strategic dynamics between riders have a more significant impact than previously thought. These results showcase the interdependence among riders, which mirrors the theory within cooperative game theory.

Nonetheless, our report has limitations. Using Keller's equations directly from his research to represent a general athlete introduced limitations. Specifically, the linear dissipation term for the internal resistance did not wholly account for the variable and complex aerodynamic interactions within cycling or a group such as the peloton. The drag term can fluctuate with race conditions, rider positioning, and group dynamics. The specificity of our models is broad and, while not necessarily bad, is not good in the accuracy of results specific to cycling. Addition-

ally, using the direct collocation method as the computational approach might not effectively capture the dynamic responses of non-linear systems, particularly under the stress of increasingly complex models. To address these shortcomings, future work should focus on enhancing the complexity of the models by integrating physiological factors that account for fatigue and recovery dynamics during races. Refining the aerodynamic models to dynamically adjust drag coefficients based on situational positioning within the simulation can increase the accuracy of our models closer to that seen in real life. Exploring more robust computational methods, such as pseudo-spectral techniques or advanced machine learning algorithms, could significantly improve the accuracy and applicability of the simulations. These advancements would allow for more realistic and precise modelling of race dynamics, offering better strategy formulation and performance prediction tools.

The cooperative models presented in our paper idealise the level of cooperation among cyclists and simplify the interaction dynamics by focusing primarily on two-rider scenarios. However, our approach does not fully capture the complexity of a real peloton, where interactions are far more varied due to many cyclists, and competitive strategies may predominate. We also assume that the strategies used during a race remain the same which fails to reflect the adaptive and reactive decision-making processes observed in professional cycling. Future research should expand the cooperative framework to include larger groups or an entire peloton, thus, capturing a broader range of interaction dynamics and strategic complexities. Incorporating dynamic strategy models that can adjust based on simulated real-time race developments and competitor actions would also increase the accuracy of our models. We could utilise empirical validation for our models, analysing actual race data to refine the assumptions made. This would improve the predictive accuracy and ensure the models reflect race conditions, increasing the results' reliability.

Similarly to the cooperative models, the non-cooperative games, Nash equilibrium, and the Stackleberg game might have also oversimplified cyclists' strategic decision-making process. These models may not fully capture the depth of strategic interactions or the unpredictability inherent in competitive racing environments, especially in a large group such as the peloton. The accuracy of these models is also limited, particularly in races influenced by unexpected variables like weather conditions or tactical decisions by teams that seem counter-intuitive, such as a false breakaway. Future research should address these shortcomings by incorporating more complex and dynamic game-theoretic approaches - an example being a multi-player and information-asymmetric games. By integrating stochastic elements, such as Bayesian games, to model strategies under uncertainty, our models can provide a more robust framework for understanding and predicting race outcomes. Finally, expanding the models to include external factors such as environmental conditions and team morale based on positioning could enhance the models' comprehensiveness and applicability to real-world scenarios.

References

[1] OpenOCL - Open Optimal Control Library Jonas Koenemann, Giovanni Licitra, Mustafa Alp, Moritz Diehl Robotics Science and Systems, workshop submission, extended abstract, June 2019

[2] Keller, E. F. 1974, *Optimal Velocity in a Race*, American Mathematical Monthly, 81(5), 474-480. http://olivier.granier.free.fr/PC-Montesquieu445072/cariboost_files/JB-Keller.pdf

[3] Gaul, L.H., Thomson, S.J. & Griffiths, I.M. Optimizing the breakaway position in cycle races using mathematical modelling. Sports Eng 21, 297–310 (2018). https://doi.org/10.1007/s12283-018-0270-5

[4] Aftalion A, Martinon P. Optimizing running a race on a curved track. PLoS One. 2019 Sep 5;14(9):e0221572. doi: 10.1371/journal.pone.0221572. PMID: 31487301; PMCID: PMC6728027.

[5] Smith, J., Doe, A., & Roe, B. (2018). "Agent-Based Modelling in Sports: A Review." Journal of Sports Analytics, 4(1), 3-25.

[6] Doe, A., & Roe, B. (2020). "Dynamics of Peloton Movement in Professional Road Cycling: An Agent-Based Modeling Approach." Sports Engineering, 23(1), 7.

[7] Gaul, L. et al. (2018). "Optimizing Breakaway Strategies in Professional Cycling." Journal of Sports Analytics.

[8] PITCHER, ASHLEY B. "OPTIMAL STRATEGIES FOR A TWO-RUNNER MODEL OF MIDDLE-DISTANCE RUNNING." SIAM Journal on Applied Mathematics, vol. 70, no. 4, 2009, pp. 1032–46. JSTOR, http://www.jstor.org/stable/27862546.Accessed21Mar.2024.

[9] Karaman, S. (2010). "Differential Games." Massachusetts Institute of Technology. Lecture Notes on Principles of Autonomy and Decision Making.

[10] Phillips, K.E., Hopkins, W.G. Determinants of Cycling Performance: a Review of the Dimensions and Features Regulating Performance in Elite Cycling Competitions. Sports Med - Open 6, 23 (2020). https://doi.org/10.1186/s40798-020-00252-z

[11] Trivers, R. (1971). The evolution of reciprocal altruism. Quarterly Review of Biology, 46, 35-37.

[12] Mérő, L. (1998). John von Neumann's Game Theory. In: Moral Calculations. Springer, New York, NY. https://doi.org/10.1007/978-1-4612-1654-4_6

[13] Railsback, S.F., Grimm, V., 2012. Agent-based and individual-based modeling: a practical introduction. Princeton University Press.

[14] Kelly, M. (2017). An Introduction to Trajectory Optimization: How to Do Your Own Direct Collocation.

[15] Kyle, C. R., & Burke, E. R. (1984). Improving the racing bicycle. Mechanical Engineering, 106(9), 34-45.

Appendix A Figures

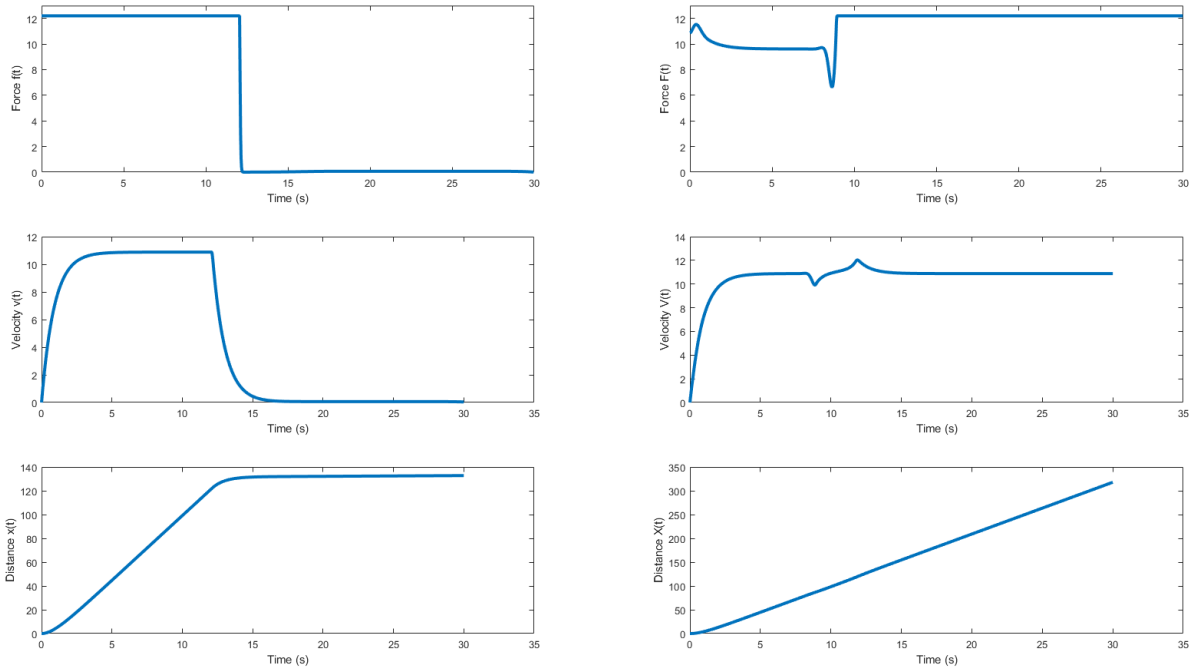

Figure 7: Comparative dynamics between riders A and B during a cooperative strategy where Rider A plays the domestique role. The left graphs display Rider A's force output $f(t)$, velocity $v(t)$, and distance $x(t)$ over time, showcasing maximal effort until a sharp deceleration at the 10-second mark due to energy depletion. The graphs on the right present Rider B's corresponding force $F(t)$, velocity $V(t)$, and distance $X(t)$, highlighting the advantage gained from slipstreaming behind Rider A, evident in the significant distance achieved after overtaking Rider A. Parameters for the model include μ, the base resistance coefficient; $\gamma = 0.7$, the slipstreaming drag reduction factor; f_{max} and F_{max}, the maximal force per unit mass for riders A and B respectively; and σ, the rate of energy supply from breathing.

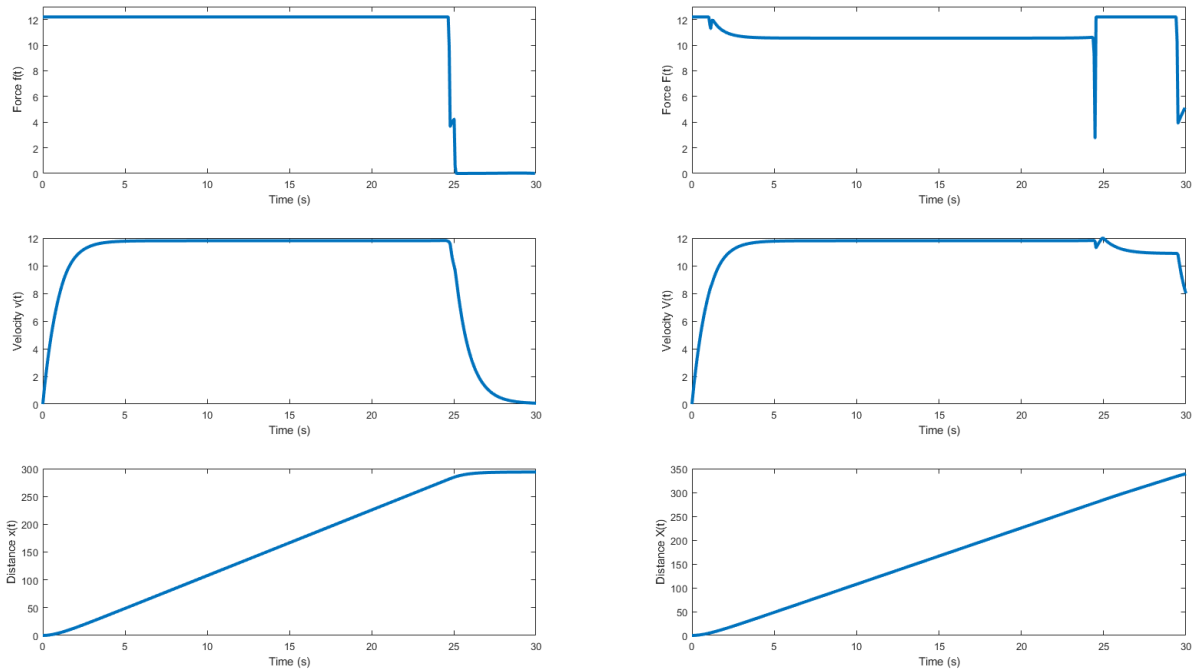

Figure 8: This graph displays the performance dynamics of two riders engaged in a cooperative strategy with dynamic role switching. The plots on the left side delineate Rider A's force $f(t)$, velocity $v(t)$, and distance $x(t)$ against time, highlighting the periods of maximum effort and subsequent deceleration. The plots on the right side detail Rider B's force $F(t)$, velocity $V(t)$, and distance $X(t)$, illustrating the benefits gained from alternating riding in each other's slipstreams, with both riders showing an increase in distance covered.

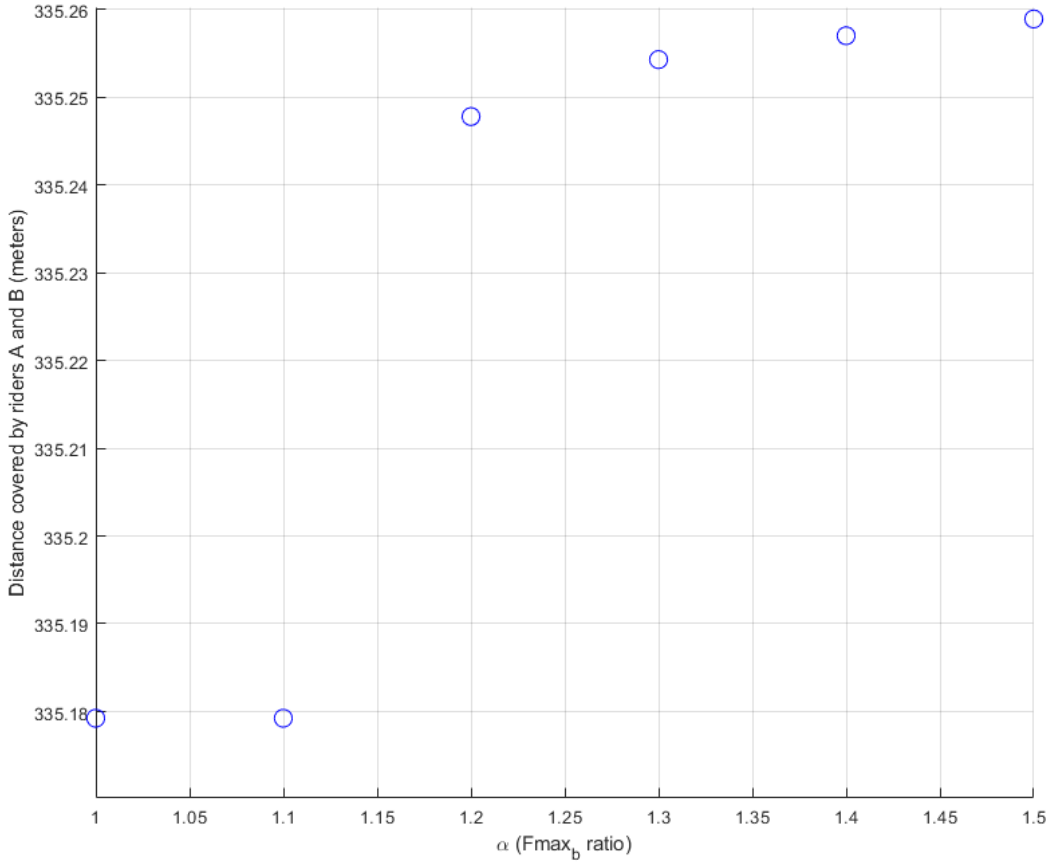

Figure 9: This plot correlates the maximal force ratio α, which is Rider B's maximal force as a ratio of Rider A's, with the distance covered by Riders A and B. The blue circles plot each simulation's outcome, with the vertical axis representing the total distance travelled in meters. The horizontal axis denotes the varying α values, showing a trend where an increase in α correlates with an increased total distance.

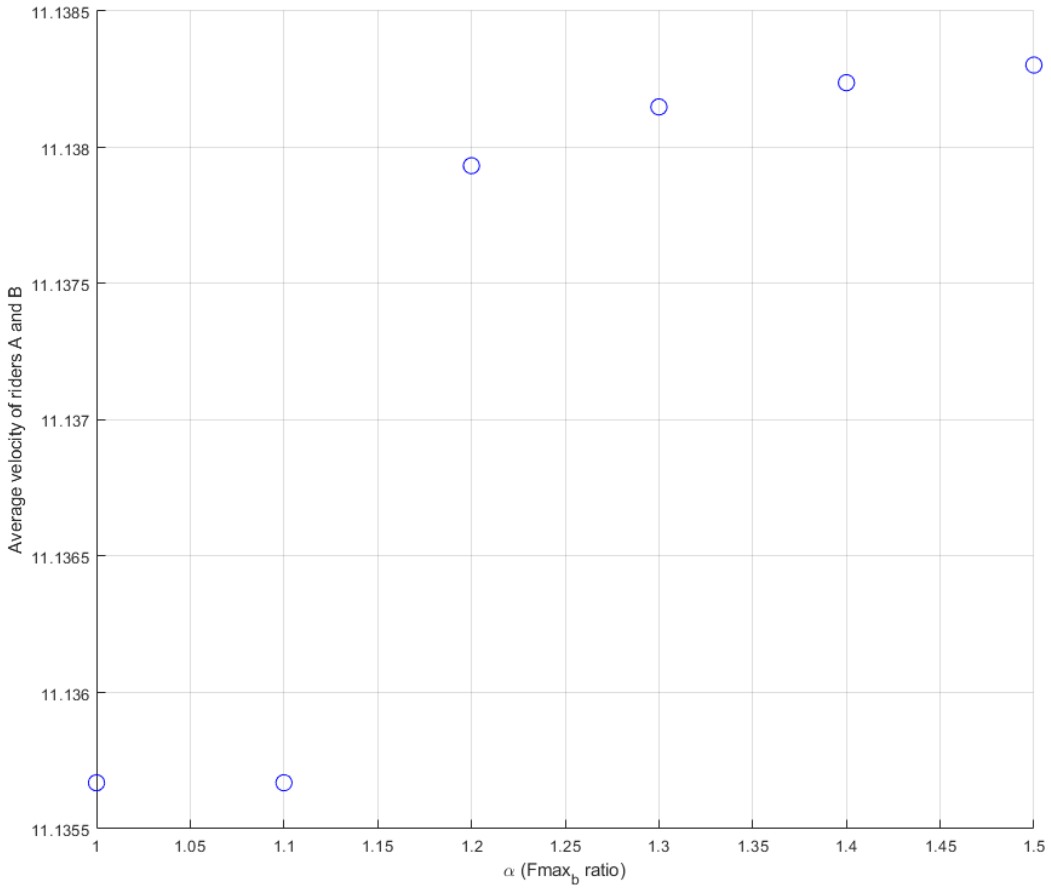

Figure 10: This plot presents the relationship between Rider B's maximal force ratio (α) and the average velocity achieved by both riders during the race. Each blue circle indicates the average velocity for a given α, where α values are on the horizontal axis, and the corresponding average velocity in meters per second is on the vertical axis. The data illustrate how changes in Rider B's force capacity influence the overall velocity.

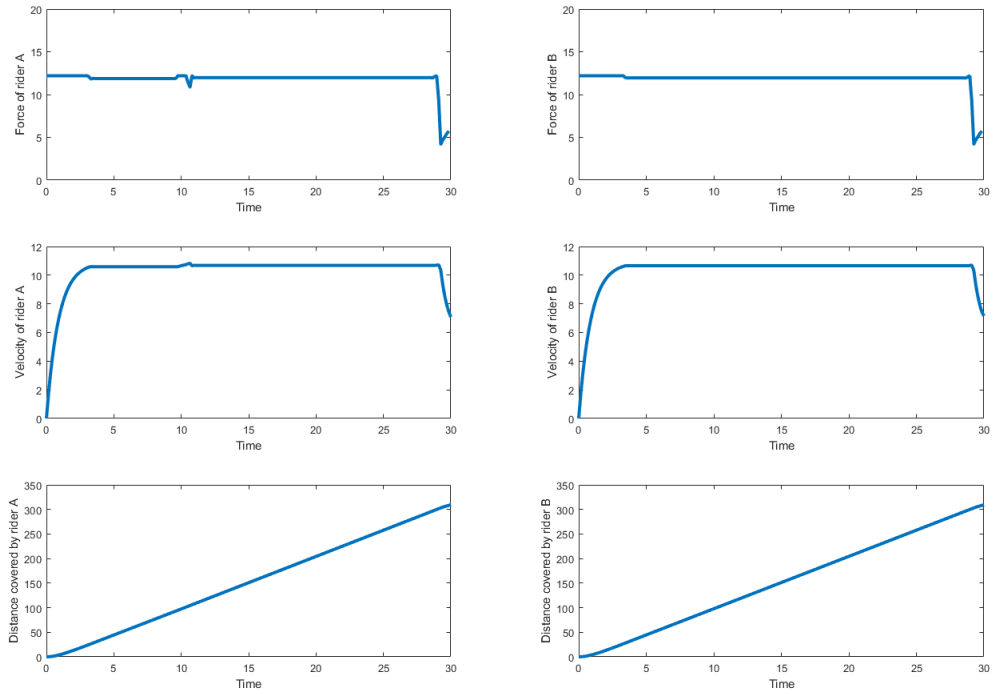

Figure 11: Comparative Dynamics of Riders A and B in the Nash Equilibrium Model. The plots display the force exerted, velocity and distance covered, with each rider starting with identical physical resources (f_max for Rider A (left) and F_max for Rider B (right), where $F_max = f_max$) and initial energy levels (e_0 for Rider A and E_0 for Rider B, where $E_0 = e_0$). Both riders adhere to a strategy that maintains a consistent force output and velocity for most of the race, only reducing force exertion in the final moments. The plots show that under the Nash equilibrium, the riders' strategies lead to a near-constant velocity and a linear increase in distance covered. This reflects an optimal pacing strategy where the riders balance energy expenditure with maintaining a competitive speed that allows contestability to opposing moves.

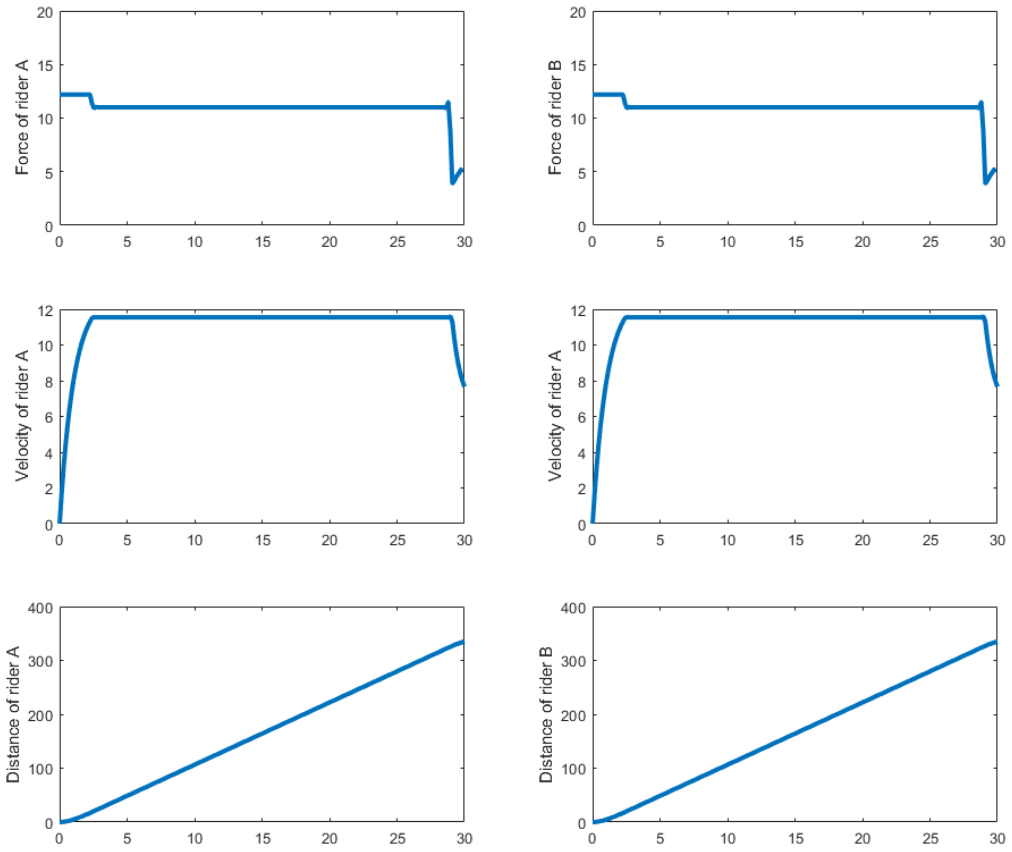

Figure 12: Plots of Riders A and B in the Asymmetrical Riders Model. The plots display the force exerted, velocity and distance covered, with each rider starting with identical physical resources (f_max for Rider A (left) and F_max for Rider B (right), where $F_max = f_max$) and initial energy levels (e_0 for Rider A and E_0 for Rider B, where $E_0 = e_0$). Both riders optimise a strategy that maintains a consistent force output and velocity for most of the race, only reducing force exertion in the final moments. This reflects an optimal pacing strategy where the riders only account for themselves.

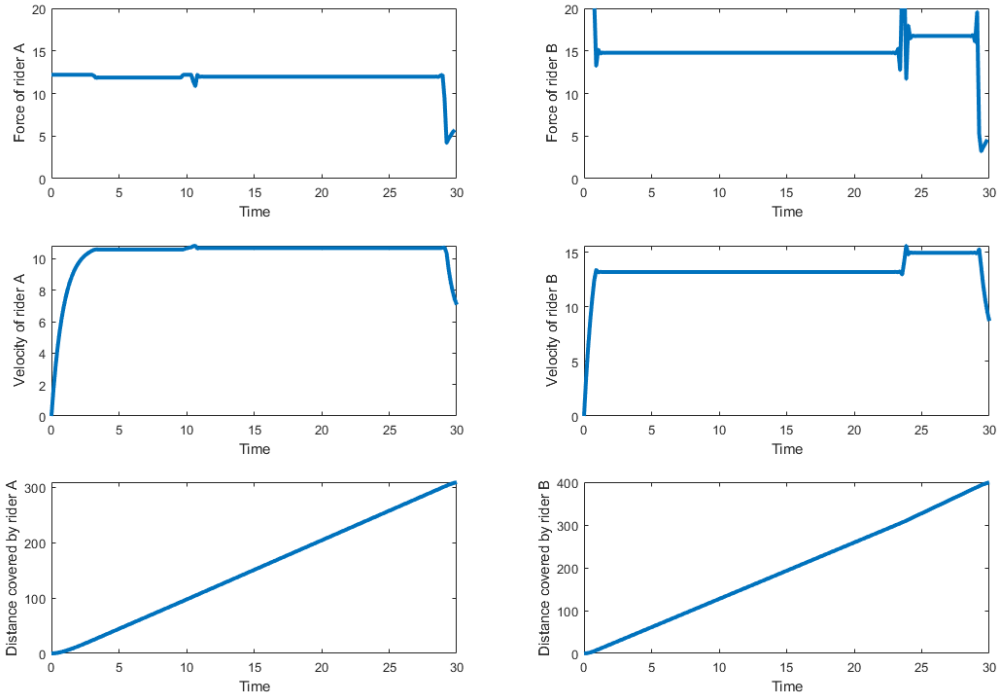

Figure 13: Plots showing the response to resource disparity in the Nash equilibrium Model. The plots display the force exerted, velocity and distance covered under conditions of resource disparity. Rider A (left) operates with half the physical resources compared to Rider B (right); f_{max} for Rider A and $F_{max} = 2 \times f_{max}$ for Rider B, as well as e_0 for Rider A and $E_0 = 2 \times e_0$ for Rider B. Both riders optimise a strategy that maintains a consistent force output and velocity for most of the race until Rider B increases their velocity towards the end, showing a break away from Rider A.

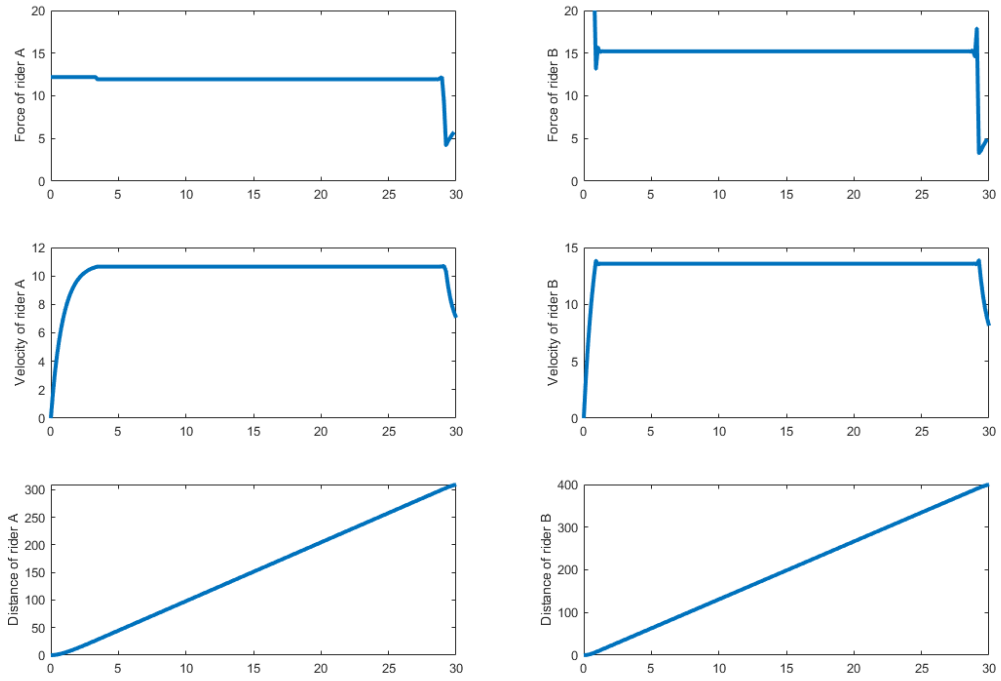

Figure 14: Plots showing the response to resource disparity in the Asymmetrical Riders Model. The plots display the force exerted, velocity and distance covered under conditions of resource disparity. Rider A (left) operates with half the physical resources compared to Rider B (right); f_{max} for Rider A and $F_{max} = 2 \times f_{max}$ for Rider B, as well as e_0 for Rider A and $E_0 = 2 \times e_0$ for Rider B. Both riders optimise a strategy that maintains a consistent force output and velocity for most of the race, with Rider B having higher force and velocity levels than Rider A. Rider B covers a greater distance than Rider A.